


 Cite this: *Chem. Commun.*, 2019, 55, 412

 Received 1st October 2018,  
 Accepted 3rd December 2018

DOI: 10.1039/c8cc07865c

rsc.li/chemcomm

## Robust multivariate metal–porphyrin frameworks for efficient ambient fixation of CO<sub>2</sub> to cyclic carbonates†

 Liang He,<sup>id</sup> ab Jayanta Kumar Nath<sup>a</sup> and Qipu Lin<sup>id</sup> \*<sup>a</sup>

**A family of multivariate metal–organic frameworks (MOFs) with three-kinds of orderly distributed metals were designed and successfully synthesized by combining metalporphyrin sheets and pentafluoride (NbOF<sub>5</sub>)<sup>2-</sup> pillars. Benefiting from the cooperative nature of open-metal-sites (OMSs) within porphyrins, specific pore-sizes, coupled with fluorine-rich electrostatic environments, the fabricated materials demonstrated high affinity toward CO<sub>2</sub>, and good catalytic performance, structural robustness, and good recyclability for the conversion of epoxides and CO<sub>2</sub> to cyclic carbonates at room temperature and 1 atm pressure.**

Anthropogenically discharged carbon dioxide (CO<sub>2</sub>) is well established to be a primary factor of global warming.<sup>1</sup> To solve this problem and recycle carbon resources, many reactions involving CO<sub>2</sub> as a C1 feedstock have been intensively developed over the past few decades.<sup>2</sup> Among them, the chemical insertion of CO<sub>2</sub> into epoxides for affording cyclic carbonates has been proposed as an attractive protocol, not only due to its 100% atom-economy but also because of the industrial potential of carbonate products for use as degreasers, electrolytes, and so on.<sup>3</sup> Thus far, lots of efforts have been devoted towards the realization of catalytic systems with extremely high reactivity and selectivity, like ionic liquids,<sup>4</sup> Schiff bases,<sup>5</sup> and metal complexes.<sup>6</sup> In particular, metalporphyrins have shown outstanding CO<sub>2</sub>-fixation performance.<sup>7</sup> However, such molecular catalysts bring forth the common issues of a homogeneous system like the intricacies of product isolation and catalyst recovery. One of the effective solutions to these drawbacks is to develop heterogeneous catalysts, like metal oxides,<sup>8</sup> zeolites,<sup>9</sup>

and polymers,<sup>10</sup> which can be readily separated and then potentially reused. However, most CO<sub>2</sub>-epoxide coupling processes catalyzed by them are still limited to elevated temperature and/or pressure, thus requiring additional cost penalties. Consequently, there is still a need to search for excellent heterocatalysts that have a high density of CO<sub>2</sub> trap-sites and catalytically-active centers.

Metal–organic frameworks (MOFs) are inherently modular, that is, amenable to crystal engineering for targeting desired structures to satisfy the dual challenge of CO<sub>2</sub> capture and fixation.<sup>11</sup> Up to now, several synthetic strategies, including creation of unsaturated metal sites and addition of organic amines, have been employed to reinforce the CO<sub>2</sub> sorption capacity of MOFs by forming chemical bonds, which results in high energy costs associated with the regeneration of sorbents.<sup>12</sup> Recently, Zaworotko and co-workers developed a group of square grid-like layers based on linked metal nodes that are pillared *via* a hexafluorosilicate to form a three-periodic network (termed SIFSIX-*n*) with a primitive cubic topology.<sup>13</sup> Benefitting from pore size control and favourable electrostatics from the periodically-lined fluorides, SIFSIX-*n* was found to offer a higher efficient trap mechanism for CO<sub>2</sub>, even in the presence of moisture.<sup>11a,14</sup> However, these isorecticular series based on linear bipyridine or its variants do not have Lewis acidic or other types of catalytically-active sites, which can further convert CO<sub>2</sub> into cyclic carbonates. To achieve a high content of catalytically-active sites in MOFs, one appealing approach is to integrate open metal sites (OMSs) or Brønsted acidic sites by judicious selection of metal nodes and/or metallolinkers.<sup>15</sup> Metalporphyrins are found in nature as biocatalysts, which are capable of activating CO<sub>2</sub>.<sup>11e,16</sup> Through ligand substitution, we have diversified the SIFSIX-*n* platform to attain a metalporphyrin-functionalized version, CPM-131, with the formula of ZnSiF<sub>6</sub>(TPyPFe).<sup>17</sup> Notably, the SIFSIX pillar could also be exchanged by a polyfluorometalate,<sup>18</sup> like (NbOF<sub>5</sub>)<sup>2-</sup>, thus fluoride–porphyrin organization permits the use of up to three types of metal ions in various combinations (including the core and peripheral coordination sites of porphyrin). Besides multivariate MOFs based on the random-location of multi-metals

<sup>a</sup> State Key Laboratory of Structural Chemistry, Fujian Institute of Research on the Structure of Matter, Chinese Academy of Sciences, Fuzhou, Fujian 350002, China. E-mail: linqipu@fjirsm.ac.cn

<sup>b</sup> College of Materials Science and Engineering, Fujian Normal University, Fuzhou, Fujian 350007, China

† Electronic supplementary information (ESI) available: Detailed experimental procedures, and additional characterization figures (SEM-EDS, FT-IR, UV-vis, TGA, thermal and chemical stability analyses, N<sub>2</sub> and CO<sub>2</sub> sorption isotherms, etc.) for the FTPFs. See DOI: 10.1039/c8cc07865c

resulting from their similar coordination preference,<sup>19</sup> to the best of our knowledge, no study has been reported on targeting hetero-trimetallic MOFs with crystallographic ordering. In view of their unique synergistic advantages, it is highly desirable to pursue new heterometallic crystalline materials.

Herein, *via* substitution of pillar/linker and node in CPM-131, we have developed a series of fluorinated trimetal-porphyrin frameworks (termed FTPFs). These are unusual examples of multivariate MOFs, constructed from copper tetrakis(4-pyridyl)-metalloporphyrin (TPyP-M) coordination (4,4)-grid layers that are pillared by the fluorometalate ( $\text{NbOF}_5$ )<sup>2-</sup>, accordingly also denoted as Cu-Nb-M (M = Zn, Fe, Ni). Bearing the optimized pore partition, OMSs in eclipse-arranged metalloporphyrins, plus electrostatic fluoropillars, these materials exhibit reversible adsorption with high capacity and affinity for CO<sub>2</sub> at 0 °C and room temperature. These FTPFs have good chemical stability in various organic solvents and tolerance to water over a wide pH range. The good adsorption capacity for CO<sub>2</sub> and high-density metalloporphyrinic OMSs make them highly efficient and reusable heterocatalysts for CO<sub>2</sub> coupling with epoxides to form cyclic carbonates under mild conditions.

Square-shaped microcrystals of FTPFs, *viz.* Cu-Nb-M (M = Zn, Fe, Ni), were prepared by layering an *N*-methyl-2-pyrrolidone solution of TPyP-M in a vial onto an ethylene glycol solution of CuNbOF<sub>5</sub>. With a size of ~1 μm, as shown in the scanning electronic microscopy (SEM) images (Fig. S3–S5, ESI†), all samples of CuNbOF<sub>5</sub>-metalloporphyrins were not suitable for structure determination by single-crystal X-ray diffraction (SCXRD). Guided by the prototype of the previously-described CPM-131, their structures with the space group *P4/mmm* were constructed by using the Reflex Plus implemented in the Materials Studio (detailed modeling in Section S3, ESI†).<sup>20</sup> For the representative Cu-Nb-Ni, the experimental powder X-ray diffraction (PXRD) pattern was indexed and compared with that refined *via* the Rietveld method, resulting in good agreement factors ( $R_p = 8.35\%$ ,  $R_{wp} = 5.62\%$ , Fig. S2, ESI†). The fitted unit cell parameters ( $a = b = 13.6484$  Å,  $c = 8.0870$  Å) are nearly consistent with those of CPM-131, but with a slightly bigger *c*-value attributed to the relatively-longer metal-fluorine distance (1.97 Å for Nb-F *versus* 1.68 Å for Si-F). As anticipated, Cu-Nb-Ni consists of CuNbOF<sub>5</sub> chains formed *in situ* running along the *c*-direction. Such infinite rod-like chains are bridged to each other through metalloporphyrinic spacers, giving rise to a 4,6-connected **fs**c-net with elliptical channels (Fig. 1), formulated as CuNbOF<sub>5</sub>(TPyPNI). Apart from the fluoride-decorated pore environment, another prominent structural aspect in FTPFs is the eclipsed array of metalloporphyrins, with an interplanar spacing equal to the *c*-axial length.

Thermogravimetric analysis (TGA) and temperature-dependent PXRD (Fig. S11 and S12, ESI†) indicated that the structure of Cu-Nb-Ni was undamaged up to 250 °C in air. Its porosity was examined using the N<sub>2</sub> adsorption-desorption isotherms at 77 K (Fig. S16–S18, ESI†). Prior to testing, the as-synthesized samples were exchanged with MeOH for 24 h and then dried at 120 °C under vacuum for 12 h to remove the remnant solvent molecules. An N<sub>2</sub> uptake of 175 cm<sup>3</sup> g<sup>-1</sup> (STP) and a

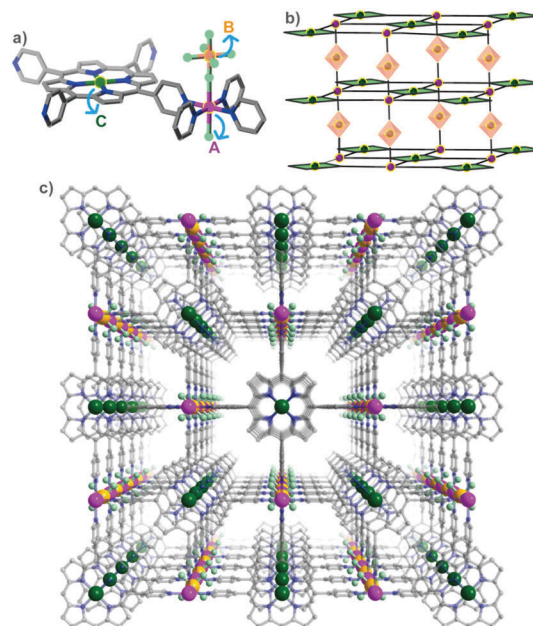


Fig. 1 (a) Local coordination environments of the three different metal sites labelled A (from  $\{M(\text{Pyridine})_4\text{F}_2\}$ ), B (from  $\{MO_xF_{6-x}\}$ ) and C (from metalloporphyrin) in different colours. (b) Network topology of the FTPFs. (c) Crystal structure of the FTPFs. H atoms are omitted for clarity.

Brunauer-Emmett-Teller (BET) surface area of 336 m<sup>2</sup> g<sup>-1</sup> (a corresponding Langmuir surface area of 905 m<sup>2</sup> g<sup>-1</sup>) were observed, which are comparable to those of CPM-131. An evaluation using the Horvath-Kawazoe model revealed a pore size distribution centered at 4.1 Å, slightly lower than 4.3 Å of CPM-131, probably due to a relatively shorter proximal distance between the adjacent fluorine centers and the consequently contracted aperture size of the channels by using a pillar with a bigger cation (Nb<sup>5+</sup> instead of Si<sup>4+</sup>). The PXRD patterns revealed that no change occurs during immersion in common solvents, such as MeOH, EtOH, DMF, (Me)<sub>2</sub>CO, MeCN, *etc.* for 24 h (Fig. S13, ESI†). Moreover, it was found that Cu-Nb-Ni can tolerate pH = 3–11 aqueous solutions (Fig. S14 and S15, ESI†). The stability of the FTPFs in these chemical conditions makes them attractive for use in certain practical applications. The hetero-trimetal coexistence in each sample was also supported by the inductively coupled plasma optical emission (ICP-OES), and energy dispersive X-ray spectroscopy (EDS) results (Fig. S6–S8, ESI†). The solid-state ultraviolet visible (UV-vis) diffuse reflectance spectra (DRS, Fig. S10, ESI†) of the materials indicated a significant effect of the porphyrinic metal sites on the electronic structure and the absorption nature.

The unique pore geometry and chemistry prompted us to evaluate the CO<sub>2</sub> capture performance of the FTPFs. Low-pressure CO<sub>2</sub> sorption data were collected at 273 and 298 K (Fig. 2b and Fig. S19, S20, ESI†). The appreciable CO<sub>2</sub> uptake of representative Cu-Nb-Ni at 1 atm and 273 K was found to be 87 cm<sup>3</sup> g<sup>-1</sup> (equivalent to 3.9 mmol g<sup>-1</sup> or 171 mg g<sup>-1</sup>), while 63 cm<sup>3</sup> g<sup>-1</sup> (equivalent to 2.8 mmol g<sup>-1</sup> or 124 mg g<sup>-1</sup>) was measured at 1 atm and 298 K, which are comparable to those of the SIFSIX-*n* series and also at the high end among porphyrin-based

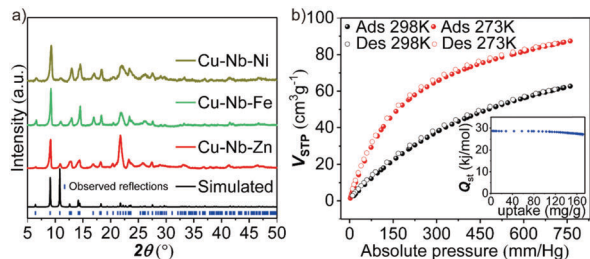


Fig. 2 (a) As-synthesized and simulated powder X-ray diffraction (PXRD) patterns for Cu–Nb–M (M = Zn, Fe, Ni). (b) CO<sub>2</sub> uptake for Cu–Nb–Ni at 273 and 298 K, respectively, with the inset showing the CO<sub>2</sub> isosteric heat of adsorption ( $Q_{st}$ ).

MOFs.<sup>11a,13b,14b,15b</sup> High affinity for CO<sub>2</sub> is shown by the sharp increase in the CO<sub>2</sub> uptake in the low pressure region, which could be attributed to the enhanced isosteric heats ( $Q_{st}$ ). The  $Q_{st}$  value was calculated by fitting the adsorption data collected at 273 and 298 K to the virial model (Fig. S21–S24, ESI†). At zero coverage, the adsorption enthalpy of CO<sub>2</sub> for Cu–Nb–Ni is 29 kJ mol<sup>-1</sup>, close to that of the other isostructural analogues (28 and 29 kJ mol<sup>-1</sup> for Cu–Nb–Fe, and Cu–Si–Fe, respectively) and SIFSIX-**pcu**-type materials, suggesting a strong interaction of CO<sub>2</sub> with the pore surface of the FTPFs. The  $Q_{st}$  was also relatively constant, indicative of homogenous energy sites over the full range of CO<sub>2</sub> loading. The results show that OMSs, fluoropillars, and small pore sizes likely contribute to the uptake and  $Q_{st}$  of CO<sub>2</sub>.

FTPFs with high CO<sub>2</sub>-trap, structural robustness, and eclipsed array of uniformly implanted active sites are ideal candidates for chemical coupling of CO<sub>2</sub> with epoxides to form cyclic carbonates. In a typical experiment at room temperature and 1 atm pressure in the presence of tetra-*n-tert*-butylammonium bromide (TBAB) as the co-catalyst, the yields of the cyclic carbonates produced from the coupling reaction of CO<sub>2</sub> with epoxides were determined by the <sup>1</sup>H NMR technique. A comparative study showed that Cu–Nb–Ni exhibited the highest catalytic efficiency and is thus described in detail (Table S2, ESI†). As shown in Fig. 3, due to the dependence of the coupling conversion on reaction time, Cu–Nb–Ni demonstrated high catalytic activity for the cycloaddition of 2-methyloxirane and CO<sub>2</sub> into 4-methyl-1,3-dioxolane-2-one carbonate at room temperature and under 1 atm CO<sub>2</sub> pressure with a yield of >99% over 48 h, which can be attributed to the synergistic effect of the catalytic OMSs of the metalloporphyrin and specific CO<sub>2</sub>-trap sites. This compares favourably to the very highest values reported for MOFs and porphyrin-based materials (Table S3, ESI†).<sup>21</sup>

We examined the scope of epoxide substrates for chemical coupling with CO<sub>2</sub> to cyclic carbonates under the similar conditions. With the increase of the substituted alkyl chain sizes of epoxides, a dramatic yet steady decrease in the yield of cyclic products was observed for Cu–Nb–Ni, as indicated by 67% formation of 4-ethyl-1,3-dioxolan-2-one (entry 5, Table S2, ESI†) and 32% formation of 4,4-dimethyl-1,3-dioxolan-2-one from 2-ethyloxirane and 2,2-dimethyloxirane (entry 6, Table S2, ESI†), respectively. This could be possibly ascribed to the limited

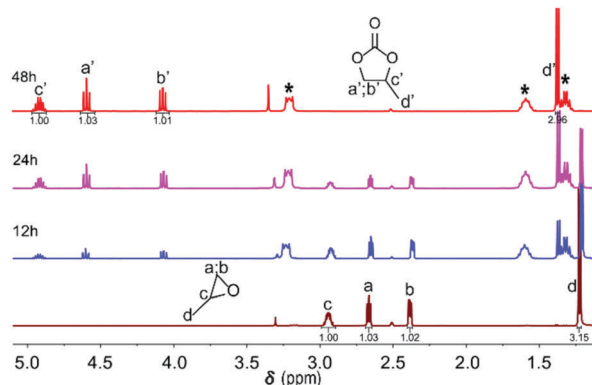


Fig. 3 <sup>1</sup>H NMR spectra before and after 12, 24, and 48 h CO<sub>2</sub> cycloaddition reaction of propylene epoxide (from bottom to top). Peaks marked with \* are for TBAB. Un-marked peaks are for solvent.

diffusion of the large-sized epoxide substrate molecules into the narrow square channel of Cu–Nb–Ni. In particular, nearly quantitative conversion of 2-(chloromethyl)oxirane to 4-chloromethyl-1,3-dioxolane-2-one was achieved over a period of 48 h (entry 4, Table S2, ESI†), further indicating the steric-hindrance effect.<sup>22</sup> In consideration of the heterogeneous nature of the FTPFs, the stability and reusability of the selected Cu–Nb–Ni were assessed by performing the cycloaddition of 2-methyloxirane with CO<sub>2</sub>. The reusability test (Fig. S28, ESI†) shows that Cu–Nb–Ni can be recycled at least four successive times with a slight decrease in the catalytic activity, and the selectivity of the product remains almost constant (>97%) during each recycling process. The PXRD result of the reused sample also confirmed that its structure showed no obvious change. This clearly verified that it is a robust catalyst candidate for CO<sub>2</sub> fixation.

Based on the above observations and some previous reports,<sup>11d,22</sup> a tentative mechanism is proposed for the cycloaddition of epoxides and CO<sub>2</sub> into cyclic carbonates catalyzed by these FTPFs. As illustrated in Fig. S29 (ESI†), the coupling reaction is initiated by binding of the epoxide with the Lewis acidic site in the metalloporphyrinic core through the formation of the M–O bond. Subsequently, nucleophilic Br<sup>-</sup> generated from TBAB attacks the less-hindered side of the coordinated epoxide to give rise to the ring-opening of the epoxy species. It should be noted that the electrostatic potential generated around the fluorides could trap CO<sub>2</sub> to primarily bind in a parallel orientation along the CuNbOF<sub>5</sub> chains, and metalloporphyrinic OMSs are also the ideal trap-site for CO<sub>2</sub>, and even can further activate CO<sub>2</sub>, which facilitates the coupling of CO<sub>2</sub> and the opened epoxy. Accordingly, an alkylcarbonate anion is formed upon interaction of CO<sub>2</sub> with the activated epoxy ring, which is then converted into the corresponding cyclic carbonate through the ring closing step. We expect that the abundance of face-to-face pairwise-oriented metalloporphyrinic OMSs could boost the synergistic effect with fluoride lined within the pore-wall and co-catalyst TBAB in the confined space, thus promoting the cycloaddition reaction, which thereby leads to high catalytic activity of FTPFs for the chemical conversion of CO<sub>2</sub> into cyclic carbonates under ambient and solvent-free conditions.

In conclusion, by a trisubstitution strategy, a novel class of ternary hetero-metallic MOFs (FTPFs) has been successfully synthesized and fully characterized. They contain (4,4)-grid-like metalloporphyrin layers that are linked by linear  $\text{Cu}^{2+}\text{-(NbOF}_5\text{)}^{2-}$  chains to form an extended porous structure. Due to the existence of a contracted pore-size, fluorine-rich channel surface, and strong Cu-F/N bonding, the resultant FTPFs are found to be robust in some common solvents including water, and also resistant to heat (up to 250 °C in air). Featuring a high density of eclipse-distributed open metal sites (OMSs) and the advantages of using the SIFSIX-analogs, these materials are demonstrated to have high  $\text{CO}_2$  trap capacities (up to ~9 wt% uptake at 273 K under 1 atm), and excellent catalytic efficiency (>99% conversion) for the chemical fixation of  $\text{CO}_2$  and epoxides with good recyclability under solvent-free conditions. Further studies will be conducted on photoelectrochemical catalysis, and the effect of decoration with a hetero-trimetal on the performance will be addressed.

This work was supported by the National Natural Science Foundation of China (Grant No. 21501028), the National Science Foundation of Fujian Province (Grant No. 2017J01039), the Strategic Priority Research Program of Chinese Academy of Sciences (Grant No. XDB20000000) and the Hundred-Talent Program of Fujian Institute of Research on the Structure of Matter, Chinese Academy of Sciences.

## Conflicts of interest

There are no conflicts to declare.

## Notes and references

- 1 M. R. Allen, D. J. Frame, C. Huntingford, C. D. Jones, J. A. Lowe, M. Meinshausen and N. Meinshausen, *Nature*, 2009, **458**, 1163.
- 2 T. Sakakura, J.-C. Choi and H. Yasuda, *Chem. Rev.*, 2007, **107**, 2365–2387.
- 3 (a) M. Mikkelsen, M. Jørgensen and F. C. Krebs, *Energy Environ. Sci.*, 2010, **3**, 43–81; (b) C. Maeda, T. Taniguchi, K. Ogawa and T. Ema, *Angew. Chem., Int. Ed.*, 2015, **54**, 134–138.
- 4 H. Kawanami, A. Sasaki, K. Matsui and Y. Ikushima, *Chem. Commun.*, 2003, 896–897.
- 5 M. Ulusoy, O. Şahin, A. Kilic and O. Büyükgüngör, *Catal. Lett.*, 2011, **141**, 717–725.
- 6 M. M. Dharman, J.-I. Yu, J.-Y. Ahn and D.-W. Park, *Green Chem.*, 2009, **11**, 1754–1757.
- 7 (a) A. Chen, Y. Zhang, J. Chen, L. Chen and Y. Yu, *J. Mater. Chem. A*, 2015, **3**, 9807–9816; (b) S. Kumar, M. Y. Wani, C. T. Arranja, J. D. A. e Silva, B. Avula and A. J. F. N. Sobral, *J. Mater. Chem. A*, 2015, **3**, 19615–19637.
- 8 H. Yasuda, L.-N. He, T. Sakakura and C. Hu, *J. Catal.*, 2005, **233**, 119–122.
- 9 (a) K. R. Thampy, J. Kiwi and M. Grätzel, *Nature*, 1987, **327**, 506; (b) M. R. Hudson, W. L. Queen, J. A. Mason, D. W. Fickel, R. F. Lobo and C. M. Brown, *J. Am. Chem. Soc.*, 2012, **134**, 1970–1973.
- 10 (a) Y. Xie, T.-T. Wang, X.-H. Liu, K. Zou and W.-Q. Deng, *Nat. Commun.*, 2013, **4**, 1960; (b) X. Zhan, Z. Chen and Q. Zhang, *J. Mater. Chem. A*, 2017, **5**, 14463–14479.
- 11 (a) P. Nugent, Y. Belmabkhout, S. D. Burd, A. J. Cairns, R. Luebke, K. Forrest, T. Pham, S. Ma, B. Space, L. Wojtas, M. Eddaoudi and M. J. Zaworotko, *Nature*, 2013, **495**, 80; (b) T. M. McDonald, J. A. Mason, X. Kong, E. D. Bloch, D. Gygi, A. Dani, V. Crocellà, F. Giordanino, S. O. Odoh, W. S. Drisdell, B. Vlaisavljevich, A. L. Dzubak, R. Poloni, S. K. Schnell, N. Planas, K. Lee, T. Pascal, L. F. Wan, D. Prendergast, J. B. Neaton, B. Smit, J. B. Kortright, L. Gagliardi, S. Bordiga, J. A. Reimer and J. R. Long, *Nature*, 2015, **519**, 303; (c) J. Song, Z. Zhang, S. Hu, T. Wu, T. Jiang and B. Han, *Green Chem.*, 2009, **11**, 1031–1036; (d) L. Liu, S.-M. Wang, Z.-B. Han, M. Ding, D.-Q. Yuan and H.-L. Jiang, *Inorg. Chem.*, 2016, **55**, 3558–3565; (e) H. He, J. A. Perman, G. Zhu and S. Ma, *Small*, 2016, **12**, 6309–6324; (f) D.-Y. Du, J.-S. Qin, S.-L. Li, Z.-M. Su and Y.-Q. Lan, *Chem. Soc. Rev.*, 2014, **43**, 4615–4632; (g) J. Chen, K. Shen and Y. Li, *ChemSusChem*, 2017, **10**, 3165–3187; (h) B. Liu, S. Yao, X. Liu, X. Li, R. Krishna, G. Li, Q. Huo and Y. Liu, *ACS Appl. Mater. Interfaces*, 2017, **9**, 32820–32828.
- 12 (a) A. Sayari, Y. Belmabkhout and R. Serna-Guerrero, *Chem. Eng. J.*, 2011, **171**, 760–774; (b) T. M. McDonald, W. R. Lee, J. A. Mason, B. M. Wiers, C. S. Hong and J. R. Long, *J. Am. Chem. Soc.*, 2012, **134**, 7056–7065; (c) S. Choi, T. Watanabe, T.-H. Bae, D. S. Sholl and C. W. Jones, *J. Phys. Chem. Lett.*, 2012, **3**, 1136–1141; (d) R. W. Flaig, T. M. Osborn Popp, A. M. Fracaroli, E. A. Kapustin, M. J. Kalmuzki, R. M. Altamimi, F. Fathieh, J. A. Reimer and O. M. Yaghi, *J. Am. Chem. Soc.*, 2017, **139**, 12125–12128; (e) Y.-Q. Lan, H.-L. Jiang, S.-L. Li and Q. Xu, *Adv. Mater.*, 2011, **23**, 5015–5020; (f) H. Wang, H. Wu, J. Kan, G. Chang, Z. Yao, B. Li, W. Zhou, S. Xiang, J. Cong-Gui Zhao and B. Chen, *J. Mater. Chem. A*, 2017, **5**, 8292–8296.
- 13 (a) S. Subramanian and M. J. Zaworotko, *Angew. Chem., Int. Ed.*, 1995, **34**, 2127–2129; (b) S. D. Burd, S. Ma, J. A. Perman, B. J. Sikora, R. Q. Snurr, P. K. Thallapally, J. Tian, L. Wojtas and M. J. Zaworotko, *J. Am. Chem. Soc.*, 2012, **134**, 3663–3666.
- 14 (a) O. Shekhah, Y. Belmabkhout, Z. Chen, V. Guillerme, A. Cairns, K. Adil and M. H. Eddaoudi, *Nat. Commun.*, 2014, **5**, 4228; (b) S. K. Elsaidi, M. H. Mohamed, H. T. Schaefer, A. Kumar, M. Lusi, T. Pham, K. A. Forrest, B. Space, W. Xu, G. J. Halder, J. Liu, M. J. Zaworotko and P. K. Thallapally, *Chem. Commun.*, 2015, **51**, 16872; (c) R.-B. Lin, L. Li, H. Wu, H. Arman, B. Li, R.-G. Lin, W. Zhou and B. Chen, *J. Am. Chem. Soc.*, 2017, **139**, 8022–8028.
- 15 (a) X. Fang, Q. Shang, Y. Wang, L. Jiao, T. Yao, Y. Li, Q. Zhang, Y. Luo and H.-L. Jiang, *Adv. Mater.*, 2018, **30**, 1705112; (b) D. Feng, Z.-Y. Gu, J.-R. Li, H.-L. Jiang, Z. Wei and H.-C. Zhou, *Angew. Chem., Int. Ed.*, 2012, **51**, 10307–10310; (c) Q. Lin, X. Bu, A. Kong, C. Mao, F. Bu and P. Feng, *Adv. Mater.*, 2015, **27**, 3431–3436; (d) J. A. Johnson, J. Luo, X. Zhang, Y.-S. Chen, M. D. Morton, E. Echeverria, F. E. Torres and J. Zhang, *ACS Catal.*, 2015, **5**, 5283–5291.
- 16 (a) C. A. Trickett, A. Helal, B. A. Al-Maythaly, Z. H. Yamani, K. E. Cordova and O. M. Yaghi, *Nat. Rev. Mater.*, 2017, **2**, 17045; (b) H. Zhang, J. Wei, J. Dong, G. Liu, L. Shi, P. An, G. Zhao, J. Kong, X. Wang, X. Meng, J. Zhang and J. Ye, *Angew. Chem.*, 2016, **128**, 14522–14526; (c) E.-X. Chen, M. Qiu, Y.-F. Zhang, Y.-S. Zhu, L.-Y. Liu, Y.-Y. Sun, X. Bu, J. Zhang and Q. Lin, *Adv. Mater.*, 2018, **30**, 1704388; (d) H.-Q. Xu, J. Hu, D. Wang, Z. Li, Q. Zhang, Y. Luo, S.-H. Yu and H.-L. Jiang, *J. Am. Chem. Soc.*, 2015, **137**, 13440–13443; (e) W.-Y. Gao, L. Wojtas and S. Ma, *Chem. Commun.*, 2014, **50**, 5316–5318.
- 17 Q. Lin, C. Mao, A. Kong, X. Bu, X. Zhao and P. Feng, *J. Mater. Chem. A*, 2017, **5**, 21189–21195.
- 18 A. Cadiau, K. Adil, P. M. Bhatt, Y. Belmabkhout and M. Eddaoudi, *Science*, 2016, **353**, 137–140.
- 19 (a) Q. Liu, H. Cong and H. Deng, *J. Am. Chem. Soc.*, 2016, **138**, 13822–13825; (b) A. Helal, Z. H. Yamani, K. E. Cordova and O. M. Yaghi, *Natl. Sci. Rev.*, 2017, **4**, 296–298.
- 20 Accelrys Materials Studio Release Notes, release 5.5.1; Accelrys Software, Inc., San Diego, CA, 2010.
- 21 (a) D. Feng, W.-C. Chung, Z. Wei, Z.-Y. Gu, H.-L. Jiang, Y.-P. Chen, D. J. Darensbourg and H.-C. Zhou, *J. Am. Chem. Soc.*, 2013, **135**, 17105–17110; (b) X. Wang, W.-Y. Gao, J. Zhang, Y. Niu, L. Wojtas, J. A. Perman, Y.-S. Chen, Z. Li, B. Aguila and S. Ma, *Chem. Commun.*, 2018, **54**, 1170–1173; (c) W.-Y. Gao, Y. Chen, Y. Niu, K. Williams, L. Cash, P. J. Perez, L. Wojtas, J. Cai, Y.-S. Chen and S. Ma, *Angew. Chem., Int. Ed.*, 2014, **53**, 2615–2619; (d) W.-Y. Gao, C.-Y. Tsai, L. Wojtas, T. Thiounn, C.-C. Lin and S. Ma, *Inorg. Chem.*, 2016, **55**, 7291–7294.
- 22 W.-Y. Gao, Y. Chen, Y. Niu, K. Williams, L. Cash, P. J. Perez, L. Wojtas, J. Cai, Y.-S. Chen and S. Ma, *Angew. Chem.*, 2014, **126**, 2653–2657.